Terminable Transitions in a Topological Fermionic Ladder

Yuchi He,[1,2] Dante M. Kennes,[1,3] Christoph Karrasch,[4] and Roman Rausch[4]

[1]*Institut für Theorie der Statistischen Physik, RWTH Aachen University
and JARA—Fundamentals of Future Information Technology, 52056 Aachen, Germany*
[2]*Rudolf Peierls Centre for Theoretical Physics, Clarendon Laboratory, Parks Road, Oxford OX1 3PU, United Kingdom*
[3]*Max Planck Institute for the Structure and Dynamics of Matter, Center for Free Electron Laser Science, 22761 Hamburg, Germany*
[4]*Technische Universität Braunschweig, Institut für Mathematische Physik, Mendelssohnstraße 3, 38106 Braunschweig, Germany*

Interacting fermionic ladders are versatile platforms to study quantum phases of matter, such as different types of Mott insulators. In particular, there are D-Mott and S-Mott states that hold preformed fermion pairs and become paired-fermion liquids upon doping (d wave and s wave, respectively). We show that the D-Mott and S-Mott phases are in fact two facets of the same topological phase and that the transition between them is terminable. These results provide a quantum analog of the well-known terminable liquid-to-gas transition. However, the phenomenology we uncover is even richer, as the order of the transition may alternate between continuous and first order, depending on the interaction details. Most importantly, the terminable transition is robust in the sense that it is guaranteed to appear for weak, but arbitrary couplings. We discuss a minimal model where some analytical insights can be obtained, a generic model where the effect persists; and a model-independent field-theoretical study demonstrating the general phenomenon. The role of symmetry and the edge states is briefly discussed. The numerical results are obtained using the variational uniform matrix-product state (VUMPS) formalism for infinite systems, as well as the density-matrix renormalization group (DMRG) algorithm for finite systems.

A ladder geometry can be thought of as a narrow strip of a two-dimensional lattice, or as a chain endowed with additional local degrees of freedom (the "rungs" of the ladder). Ladders that host interacting fermions are versatile flagship platforms for studying quantum phases and their transitions in one dimension [1–6], such as repulsion-induced pairing [7–14]; or serve as realizations of symmetry-protected topological phases [15–21]. Ladder models also appear for two-orbital chains [22,23] and effectively for more general quasi-one-dimensional systems, such as nanoribbons [24] and nanotubes [3,25–28].

A particularly interesting aspect is that fermionic ladders realize Anderson's mechanism for superconductivity from repulsive interactions, which was originally proposed for cuprates [11,29]: An effective exchange interaction at half filling causes fermions to pair up as spin singlets in an insulating Mott phase; these preformed pairs become mobile upon doping. While the physics of cuprates has turned out to be more complicated, the finite extension of the rungs of a ladder strongly favors such a pairing with a particularly strong binding energy [11]. Two pairing patterns can occur on a rung (see Fig. 1): If local repulsion dominates, it avoids double occupancy and promotes singlets across the rung. If local attraction dominates, it favors double occupancy and promotes on-site singlets. Upon doping, these patterns yield superconducting states that have been dubbed "d wave" and "s wave," respectively, in analogy to the 2D case [1,6]. The half-filled
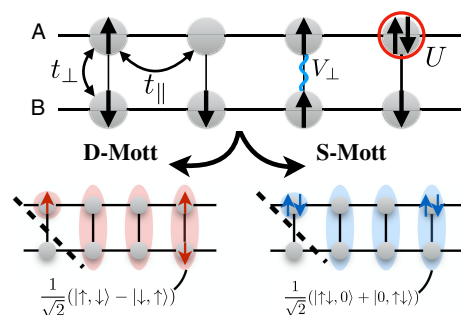

FIG. 1. Top: Illustration of our minimal ladder model, Eq. (1). Bottom: The idealized wave functions of the D-Mott (S-Mott) phase are given by product states of rung singlets (on-site singlets) in the limit of strong local repulsion $U > 0$ (strong local attraction $U < 0$). For open boundary conditions that cut the singlets open (dotted line), edge states are produced that have spin (charge) degrees of freedom. The S-Mott state can be equally achieved by a strong intrarung repulsion $V_\perp > 0$.
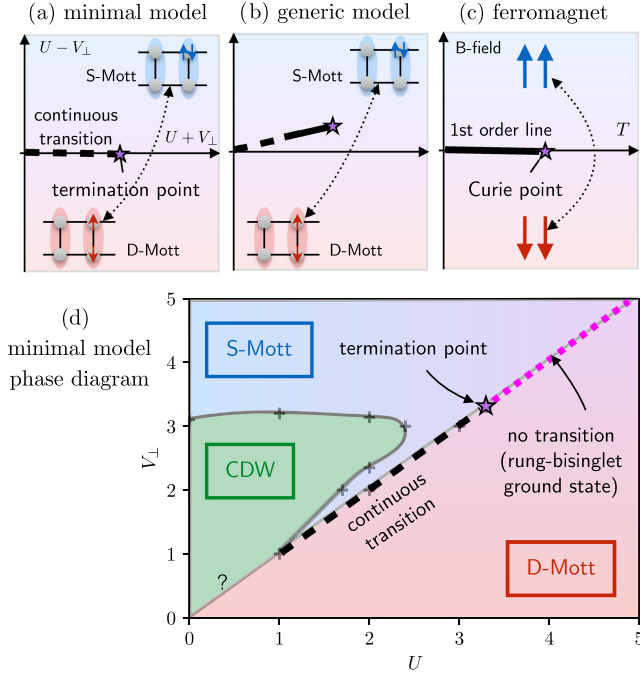
FIG. 2. (a),(b) Terminable transitions (schematic) of the fermionic ladder. The D-Mott and S-Mott (cf. Fig. 1) can be adiabatically connected via a path that avoids the transition line. The transition can be tuned to be partially first order for the generic model. (c) Paradigm of a terminable transition: a ferromagnet with a B field at finite temperature T. Below the Curie point, there is a first-order transition when tuning B across zero, but no transition above it. The phases are characterized by (a),(b) density difference of D-type and S-type singlets [Eq. (5)]; (c) density difference of $\uparrow$ and $\downarrow$ spins, i.e., magnetic moments. (d) Quantitative phase diagram for the model Eq. (1) for the minimal model, computed by VUMPS. For small interactions, it is unclear if there is a direct transition between D-Mott and CDW marked by "?." The continuous transition terminates at $U = V_\perp \approx 3.4$, after which the gapped exact rung-bisinglet (see text) is the ground state (magenta line). Different scenarios of the transition for the generic model are shown in Fig. 4.

insulating states are correspondingly called "D-Mott" and "S-Mott" [4,6]. It is known that the rung-singlet wave function (D-Mott) is a realization of the topological Haldane phase [15,18,19,22].

In this work, we study the competition between the two singlet types in more detail and find that a phase transition emerges between the two Mott states, *but the transition line is terminable.* Therefore, D-Mott and S-Mott are adiabatically connected, and one should think of them as *two facets of one and the same topological phase.* This physics also provides a quantum analog of the prototypical, classical liquid-to-gas transition, which is terminable and of first order (another example is the ferromagnet, cf. Fig. 2). However, we show that the terminable transition in our system is robust in the sense that it is guaranteed to appear at weak, but arbitrary interactions. Furthermore, its order can change from first order to second, depending on the

interaction details. This is schematically summarized in Fig. 2. As the effective theory of liquid-to-gas transitions Ref. [30] was integral to understanding the physics of a wide range of very different systems [31–37], understanding the robustness and order change of the transition line might take a similarly pronounced role.

Hamiltonian.—As a minimal model to observe the phenomenon, we consider the following Hamiltonian of fermions on a ladder (pictorially shown in Fig. 1):

$$H_{\min} = H_0 + H_{\mathrm{Hub}} + H_{\mathrm{ext}}, \qquad (1)$$

with

$$H_0 = -t_\parallel \sum_{j,l,\sigma} c^\dagger_{j+1,l,\sigma} c_{j,l,\sigma} - t_\perp \sum_{j,\sigma} c^\dagger_{j,A,\sigma} c_{j,B,\sigma} + \mathrm{H.c.},$$

$$H_{\mathrm{Hub}} = \frac{U}{2} \sum_{j,l} \Delta n_{j,l} \Delta n_{j,l}; \qquad H_{\mathrm{ext}} = V_\perp \sum_j \Delta n_{j,A} \Delta n_{j,B}, \quad (2)$$

where $c_{j,l,\sigma}$ ($c^\dagger_{j,l,\sigma}$) annihilates (creates) a fermion with spin σ at the site j of the leg $l = A, B$ of the ladder; $\Delta n_{j,l} = n_{j,l} - 1 = \sum_\sigma c^\dagger_{j,l,\sigma} c_{j,l,\sigma} - 1$ is the density deviation from half filling.

The parameters are as follows: $t_\parallel$ ($t_\perp$) is the hopping amplitude along the legs (rungs) of the ladder; similarly $V_\perp$ is the nearest-neighbor Coulomb interaction along the rungs; U is the local Coulomb interaction. We set $t_\perp = t_\parallel = 1$ and look at a repulsive $U > 0$. While local pairing in the S-Mott phase is commonly discussed in the attractive case $U < 0$, it can also be achieved by setting $V_\perp > 0$ [6] (see Fig. 1). Doing so allows us to study the competition between the two pairing patterns in the U–$V_\perp$ phase diagram without switching off the interaction.

The minimal model allows us to understand the physics most clearly. For ultracold atoms in optical lattices, it is similar to the periodic Anderson model and we believe that both can be realized with equal effort [38]. On the other hand, longer-ranged Coulomb interactions [26] and Hund's rule spin exchange $J_\perp < 0$ [39,40] are relevant in materials. To this end, we also study a generic Hamiltonian given by

$$H_{\mathrm{gen}} = H_0 + H_{\mathrm{Hub}} + H_{\mathrm{ext}} + H'_{\mathrm{ext}}, \qquad (3)$$

with

$$H'_{\mathrm{ext}} = V_\parallel \sum_{j,l} \Delta n_{j,l} \Delta n_{j+1,l} + V'_\perp \sum_j (\Delta n_{j,A} \Delta n_{j+1,B} + \mathrm{H.c.})$$

$$+ V'_\parallel \sum_{j,l} \Delta n_{j,l} \Delta n_{j+2,l} + J_\perp \sum_l \mathbf{S}_{j,A} \cdot \mathbf{S}_{j,B}, \qquad (4)$$

where $\mathbf{S}_{j,l}$ is the vector of spin operators. For carbon nanotubes, the parameters $V_\parallel \approx V_\perp$, $t_\parallel \approx t_\perp$ are expected to be only slightly anisotropic [3,28]. For chemical ladders

and two-band systems, they constitute different overlaps and may show stronger anisotropy [39–44]. Orbital nematicity may also contribute to anisotropy [45].

To solve the model, we employ the *variational uniform matrix product state* (VUMPS) formalism [46–50], which variationally determines the ground state within the class of matrix-product states in the thermodynamic limit. The central control parameter is the "bond dimension" χ, which reflects the number of variational parameters. This method is able to find ground states of gapped 1D systems to very high accuracy. We exploit the spin-$SU(2)$ and charge-$U(1)$ symmetry of the underlying problem [51], which allows us to reach bond dimensions of up to $\chi \sim 10^4$ in difficult small-gap regions. To look at edge states, we employ the related density-matrix renormalization group (DMRG) algorithm for finite systems [48,52].

Various aspects of this model family have been studied in different parameter regimes. For $V_\perp = 0$, the main focus has been on the d-wave pairing [7–10,12,14,53–56], but also on the excitations [57,58] and the topological properties [15–18]. For $V_\perp \neq 0$ and $V_\parallel \neq 0$, the onset of charge order was studied [59,60]. With analytical methods, phase diagrams have been proposed for various parameter ranges [3–6,61,62]. However, the termination of the D-Mott and S-Mott transition and the physics surrounding it have not been revealed in these works.

Microscopic characterization of S-Mott and D-Mott.— To characterize S-Mott and D-Mott, we introduce a microscopic order parameter, namely, the "singlet density difference" $\langle O_j \rangle$:

$$O_j = n_{\mathrm{D}j} - n_{\mathrm{S}j} = \Delta_{\mathrm{D}j}^\dagger \Delta_{\mathrm{D}j} - \Delta_{\mathrm{S}j}^\dagger \Delta_{\mathrm{S}j},$$
$$\Delta_{\mathrm{D}j} = (c_{j,A,\uparrow} c_{j,B,\downarrow} + c_{j,B,\uparrow} c_{j,A,\downarrow})/\sqrt{2},$$
$$\Delta_{\mathrm{S}j} = (c_{j,A,\uparrow} c_{j,A,\downarrow} + c_{j,B,\uparrow} c_{j,B,\downarrow})/\sqrt{2}. \quad (5)$$

This is motivated by the picture that D-Mott and S-Mott phases host immobile preformed d- and s-wave pairs [4], which are characterized by cross-rung pairing (D) and on-site pairing (S) [1] (cf. Fig. 1). The corresponding pair annihilation operators are $\Delta_{\mathrm{D}j}$ and $\Delta_{\mathrm{S}j}$. In the strongly coupled limit of independent rungs, the prototype states can be constructed as $|\mathrm{D}\rangle = \prod_j \Delta_{\mathrm{D}j}^\dagger |\Omega\rangle$ and $|\mathrm{S}\rangle = \prod_j \Delta_{\mathrm{S}j}^\dagger |\Omega\rangle$ [6], where $|\Omega\rangle$ is the vacuum state (see Fig. 1). Therefore, $\langle O_j \rangle > 0 \,(< 0)$ measures that there are more rung (local) singlets in the admixture of the wave function and we expect a sign change across the phase transition.

Results for the minimal model Eq. (1).—The full phase diagram obtained numerically is shown in Fig. 2. We find a phase transition line between D-Mott and S-Mott along $U = V_\perp$, which remarkably terminates at $U = V_\perp \approx 3.4$. The continuous transition is detected [Fig. 3(a)] via a divergence of the correlation length ξ in the thermodynamic limit, extrapolated using VUMPS data [63,64]. (A direct
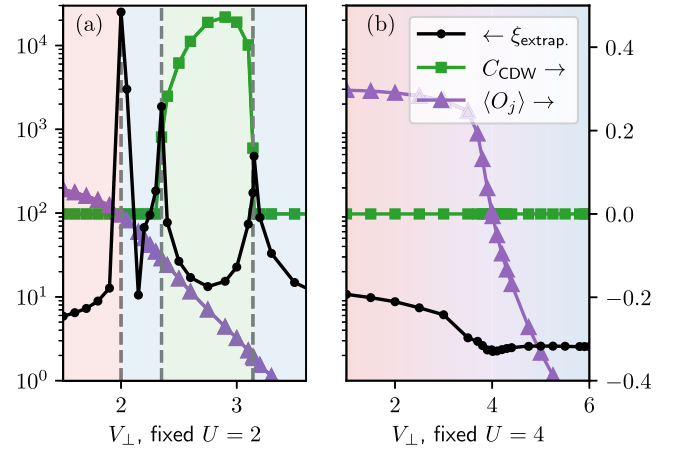

FIG. 3. Extrapolated correlation lengths (left scale) and order parameters (right scale) along (a) $U = 2$; (b) $U = 4$ for the minimal model Eq. (1). Charge density wave order parameter: $C_{\mathrm{CDW}} = 1/2 |\langle n_{j,A} \rangle - \langle n_{j,B} \rangle|$. For the definition of $\langle O_j \rangle$, see Eq. (5).

computation of the gap for finite systems yields consistent results [64]). The region with the charge density wave (CDW) is irrelevant to our discussion. Our data show no gap closing and no obvious discontinuity for large U [cf. $U = 4$ in Fig. 3(b)], implying that there is an adiabatic path connecting the two Mott phases.

The minimal model has an artifact, namely, the accidental conservation of particle number in the subband basis for $U = V_\perp$. This enables us to analytically locate the transition exactly along the $U = V_\perp$ line and track its termination. We will later show that the existence of a continuous transition is robust without the need for an accidental symmetry. Introducing the transverse subband basis $c_{j,k_y,\sigma}$ as $c_{j,0,\sigma} = (c_{j,A,\sigma} + c_{j,B,\sigma})/\sqrt{2}$ and $c_{j,\pi,\sigma} = (c_{j,A,\sigma} - c_{j,B,\sigma})/\sqrt{2}$, where $k_y = 0, \pi$ is the transverse momentum, we can rewrite the Hamiltonian Eq. (1) in this basis:

$$H_{\mathrm{min}} = -t_\parallel \sum_{j,k_y,\sigma} (c_{j,k_y,\sigma}^\dagger c_{j+1,k_y,\sigma} + \mathrm{H.c.}) - t_\perp \sum_j (n_{j,\pi} - n_{j,0})$$
$$+ U/2 \sum_j (\Delta n_{j,\pi} + \Delta n_{j,0})^2 - (U - V_\perp) H_{\mathrm{res}}, \quad (6)$$

where $n_{j,k_y} = \sum_\sigma c_{j,k_y,\sigma}^\dagger c_{j,k_y,\sigma}$. The residual term $\propto H_{\mathrm{res}}$ vanishes for $U = V_\perp$, so that $N_\pi = \sum_j n_{j,\pi}$ and $N_0 = \sum_j n_{j,0}$ become conserved. The Lieb-Schultz-Mattis theorem [65,66] states that for a fractional filling factor, the system must be gapless as long as there is no spontaneous breaking of translational symmetry. Our numerics show that the filling ratios $\langle n_{j,\pi} \rangle$ and $\langle n_{j,0} \rangle$ are fractional along $U = V_\perp$ below the termination point. Above the termination point, the fillings are integer with $\langle n_{j,\pi} \rangle = 0$ and
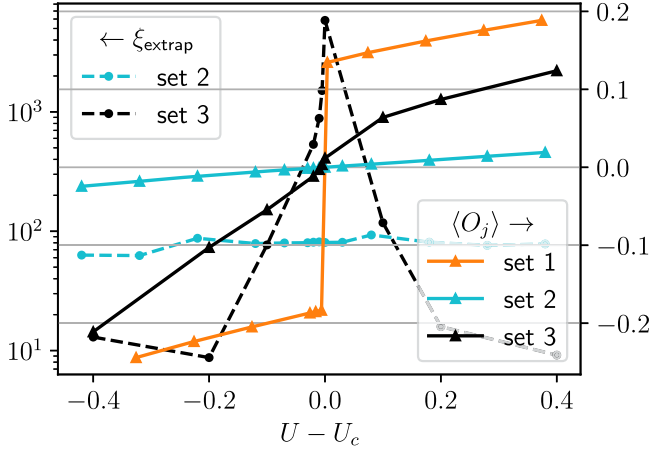
FIG. 4. Ground-state expectation $\langle O_j \rangle$ (right scale) and extrapolated correlation lengths (left scale) for the generic model Eq. (3) and the following datasets: (1) $t_\perp = 1.1$, $V_\perp = 2.88$, $V_\parallel = 2.4$, $V'_\perp = 1.92$, $V'_\parallel = 1.28$, $J_\perp = 0$ ($U_c \approx 4.426$) (2) $t_\perp = 1.1$, $V_\perp = 0.8$, $V_\parallel = 0.7$, $V'_\perp = 0.4$, $V'_\parallel = 0$, $J_\perp = -0.6$ ($U_c \approx 1.52$) (3) $t_\perp = 1.1$, $V_\perp = 2.45$, $V_\parallel = 0.5$, $V'_\perp = 0.4$, $V'_\parallel = 0.3$, $J_\perp = 0$ ($U_c \approx 2.5$), exemplifying a first-order transition, no transition, and a continuous transition, respectively.

$\langle n_{j,0} \rangle = 2$, supporting the termination of the phase transition line. The data are given in the Supplemental Material [64]. Moreover, we find numerically that the ground state above the termination point is given by a product state of equal-weight superpositions of the two singlet types: $\prod_j 1/\sqrt{2}(\Delta_{Sj}^\dagger + \Delta_{Dj}^\dagger)|\Omega\rangle$, which we dub "rung bisinglet" (cf. Fig. 2). It is straightforward to show analytically that this is an exact eigenstate of the minimal model for $U = V_\perp$. The rung bisinglet can be taken as a simple reference wave function for both the S-Mott and the D-Mott, similar to how the Affleck-Kennedy-Lieb-Tasaki (AKLT) state [67] is taken as a simple reference wave function for the Haldane phase of the $S = 1$ spin chain.

Results for the generic model Eq. (3).—The above accidental symmetry is lifted for generic interactions. The parameter space now becomes quite large and competition from other phases increases. Nevertheless, in Fig. 4, we show exemplary cases that illustrate different scenarios: The transition now may become first-order, exhibiting a jump in $\langle O_j \rangle$, but remains continuous for other parameters. We also find instances without a transition. Thus, numerical evidence indicates that the terminable transition is generic, both for nearly isotropic and anisotropic interactions.

General effective field theory.—We present an effective theory of the S-D Mott transition, which demonstrates (i) that the continuous transition line is robust beyond the accidental symmetry of the minimal model; (ii) its potential instability to first order for strong interaction; and (iii) its termination.

We use the bosonization approach and ensure that the exact accidental subband symmetry is generically absent. The bosonization of continuum operators corresponding to those of Eq. (6) are given by $c_{k_y,\sigma}(x_j) = (\kappa_{k_y,\sigma}/\sqrt{2\pi}) \sum_{\eta=-1,1} e^{i[\theta_{k_y,\sigma} + \eta(\phi_{k_y,\sigma} + k_{F,k_y\sigma}x_j)]}$, where $\theta_{k_y,\sigma}(x_j)$ and $\phi_{k_y,\sigma}(x_j)$ are dual to each other satisfying $[\theta_{k_y,\sigma}(x,t), \phi_{k'_y,\sigma'}(x',t)] = i\pi\delta_{k_y,k'_y}\delta_{\sigma,\sigma'}\Theta(x-x')$; $\{\kappa_{k_y,\sigma}, \kappa_{k'_y,\sigma'}\} = 2\delta_{k_y,k'_y}\delta_{\sigma,\sigma'}$. The $k_{F,k_y,\sigma}$ is the base wave vector of the low-energy excitation of $c_{j,k_y,\sigma}$. The half-filling condition fixes $k_{F,0,\sigma} + k_{F,\pi,\sigma} = \pi$, where $k_{F,k_y,\sigma}$ is influenced by interaction besides $t_\parallel$ and $t_\perp$. Two-band bosonization requires partially filled subbands ($k_{F,k_y,\sigma} \neq 0, \pm\pi$). Introducing a transformed basis for the effective fields: $\tilde{\phi}_{c,\pm} = \frac{1}{2}[(\phi_{0,\uparrow} + \phi_{0,\downarrow}) \pm (\phi_{\pi,\uparrow} + \phi_{\pi,\downarrow})]$ and $\tilde{\phi}_{s,\pm} = \frac{1}{2}[(\phi_{0,\uparrow} - \phi_{0,\downarrow}) \pm (\phi_{\pi,\uparrow} - \phi_{\pi,\downarrow})]$, S-Mott and D-Mott have been defined [4,6] as $\tilde{\phi}_{c,+}$, $\tilde{\phi}_{s,+}$, $\tilde{\phi}_{s,-}$ all locked at 0, and $\tilde{\theta}_{c,-}$ locked at 0 and $\pi/2$ mod π, respectively.

We now show the transition line is Gaussian-critical where O_j has quasi-long-range order and its scaling dimension indicates the instability of Gaussian criticality to a first-order transition when removing the accidental symmetry. When the sectors other than $(c,-)$ are kept locked, we can approximate the locked fields as constant and obtain

$$O_j \propto -\cos[2\tilde{\theta}_{c,-}(x_j)], \tag{7}$$

whose expectation values flip sign when the locking value $\tilde{\theta}_{c,-} = 0$ changes to $\pi/2$. The discreteness of locking values is related to time-reversal symmetry, as terms like $\cos[2\tilde{\theta}_{c,-}(x_j) + \alpha]$ with continuous varying α are forbidden by it [64]. Near the Gaussian criticality, the effective Hamiltonian density, neglecting higher harmonics, is

$$\mathcal{H}_{c,-} = \frac{v_{c,-}}{2\pi}\left[K(\partial_x\tilde{\theta}_{c,-})^2 + \frac{1}{K}(\partial_x\tilde{\phi}_{c,-})^2\right] + g\cos(2\tilde{\theta}_{c,-}), \tag{8}$$

where K is the Luttinger parameter and $g \propto (V_\perp - U)$ for the minimal model (in the generic case the relation is not known exactly). Equations (7) and (8) can be used to predict the correlator $\langle O_j O_{j+d} \rangle \propto 1/|d|^{2/K}$ at the criticality ($g = 0$). The scaling dimension of O_j is thus $1/K$. Observing nonuniversal exponents numerically confirms Gaussian criticality. For example, our minimal-model data [64] suggest that $1/K$ goes down from $\sim$0.96 to $\sim$0.46 when increasing $U = V_\perp$ from 2 to 3.2. As the 0-loop renormalization group relevance criterion is to have a scaling dimension < 2, the measured $1/K$ is consistent with this as long as $g \neq 0$ and $\tilde{\theta}_{c,-}$ gets locked.

The stability of the Gaussian transition is controlled by higher harmonic terms like $\cos(4\tilde{\theta}_{c,-})$ ($\sim O^2$); it generically
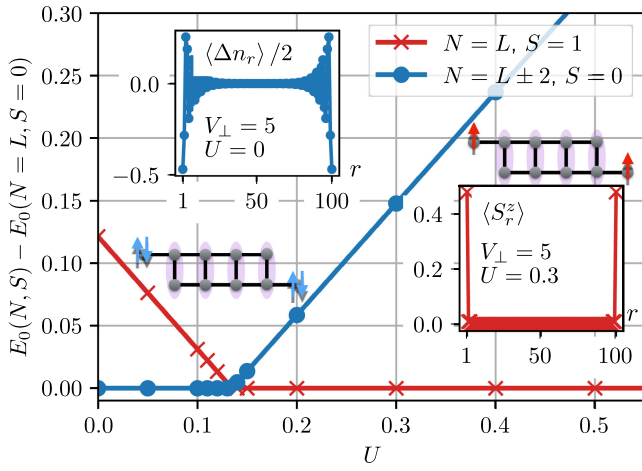
FIG. 5. Ground-state degeneracy and edge modes of open ladders under diagonal cuts. Parameters: number of sites $L = 100$ (i.e., 50 rungs), $V_\perp = 5$ in the minimal model Eq. (1). The index $r = 2j + l$ ($l = 0, 1$) consecutively labels the L sites. $E_0(N, S)$ is the lowest energy with N particles and total spin S. The insets show that the edge modes carry spin and charge quantum numbers, respectively. Upper left inset: Particle density $1/2\langle \Delta n_r \rangle = 1/2(\sum_\sigma \langle c_{r,\sigma}^\dagger c_{r,\sigma} \rangle - 1)$ in the $N = L - 2$, $S = 0$ sector. Lower right inset: spin density $\langle S_r^z \rangle = 1/2(\langle n_{r,\uparrow} \rangle - \langle n_{r,\downarrow} \rangle)$ in the $N = L$, $S = 1$ sector.

exists in the "bare" Hamiltonian, contributing to Eq. (8) and does not generically vanish simultaneously with $\cos(2\tilde{\theta}_{c,-})$ unless there is an exact subband $U(1)$ symmetry. Stable Gaussian criticality requires that those terms are irrelevant, the criterion for which is $1/K > 1/2$. This condition is always satisfied near the weak coupling limit where $1/K \to 1$, far from the marginal value, so the continuous transition is robust. Depending on model details, a perturbing interaction may induce an instability. For example, we could add some longer-ranged interaction terms as in Eq. (3), and reach $1/K$, which is small enough to induce a first-order transition described by a Landau-Ginzburg theory with powers of O, which can describe the transition termination.

Edge modes.—With a diagonally cut edge (cf. Fig. 1), the repulsive Hubbard ladder ($U > 0$, no other interactions) is known to host spin-1/2 edge modes protected by particle-hole symmetry [15,18,19]. We find that for our extended model, edge modes can carry either spin or charge quantum numbers, transforming differently under time-reversal symmetry. Intuitively, if on-site singlets (S-Mott) are cut, empty or doubly occupied sites with particle number $N = \pm 2$ remain (see Fig. 5). A change of edge quantum numbers is induced when varying the interaction parameters U and $V_\perp$. From the model wave function, one might naively assume that the edge quantum number is directly related to the bulk being D-Mott or S-Mott (i.e., to the sign of $\langle O_j \rangle$), but this is not the case: We find that spinful edge states are strongly preferred, except for very small U. For example, for $V_\perp = 5$,

a change in quantum numbers already occurs at $U \approx 0.14$ (see Fig. 5), far away from the bulk crossover $U = V_\perp$. Thus, our system provides an example where an edge transition has no bulk indication [68]; though further details are beyond the scope of this study.

Discussion.—We have shown that D-Mott and S-Mott are two facets of the same topological phase. An intuitive explanation is that true d-wave symmetry can only be found on the full 2D square lattice [69]. A robust terminable transition nevertheless exists without fine-tuning and can be understood with the help of the concept of singlet-density difference and an effective theory. Continuous transitions can be revealed experimentally by thermal conductivity peak with charge and spin transport less influenced. The existence of a robust transition itself is assisted by time-reversal symmetry, which sheds light on the study of robust terminable transitions [68]. We propose that our effective theory may be useful in discovering very different systems with similar unconventional transition behavior.

[1] T. Giamarchi, *Quantum Physics in One Dimension*, International Series of Monographs on Physics (Clarendon Press, Oxford, 2004).

[2] E. Dagotto and T. M. Rice, Surprises on the way from one- to two-dimensional quantum magnets: The ladder materials, Science **271**, 618 (1996).

[3] L. Balents and M. P. A. Fisher, Weak-coupling phase diagram of the two-chain Hubbard model, Phys. Rev. B **53**, 12133 (1996).

[4] H.-H. Lin, L. Balents, and M. P. A. Fisher, Exact SO(8) symmetry in the weakly-interacting two-leg ladder, Phys. Rev. B **58**, 1794 (1998).

[5] C. Wu, W. V. Liu, and E. Fradkin, Competing orders in coupled Luttinger liquids, Phys. Rev. B **68**, 115104 (2003).

[6] M. Tsuchiizu and A. Furusaki, Generalized two-leg Hubbard ladder at half filling: Phase diagram and quantum criticalities, Phys. Rev. B **66**, 245106 (2002).

[7] E. Dagotto, J. Riera, and D. Scalapino, Superconductivity in ladders and coupled planes, Phys. Rev. B **45**, 5744 (1992).

[8] R. M. Noack, S. R. White, and D. J. Scalapino, Correlations in a two-chain Hubbard model, Phys. Rev. Lett. **73**, 882 (1994).

[9] R. M. Noack, S. R. White, and D. J. Scalapino, The doped two-chain Hubbard model, Europhys. Lett. **30**, 163 (1995).

[10] R. M. Noack, N. Bulut, D. J. Scalapino, and M. G. Zacher, Enhanced $d_{x^2-y^2}$ pairing correlations in the two-leg Hubbard ladder, Phys. Rev. B **56**, 7162 (1997).

[11] S. Chakravarty and S. A. Kivelson, Electronic mechanism of superconductivity in the cuprates, C_{60}, and polyacenes, Phys. Rev. B **64**, 064511 (2001).

[12] Y. Gannot, Y.-F. Jiang, and S. A. Kivelson, Hubbard ladders at small u revisited, Phys. Rev. B **102**, 115136 (2020).

[13] Y.-H. Zhang and A. Vishwanath, Pair-density-wave superconductor from doping Haldane chain and rung-singlet ladder, Phys. Rev. B **106**, 045103 (2022).

[14] S. Hirthe, T. Chalopin, D. Bourgund, P. Bojović, A. Bohrdt, E. Demler, F. Grusdt, I. Bloch, and T. A. Hilker, Magnetically mediated hole pairing in fermionic ladders of ultracold atoms, Nature (London) **613**, 463 (2023).

[15] P. Sompet, S. Hirthe, D. Bourgund, T. Chalopin, J. Bibo, J. Koepsell, P. Bojović, R. Verresen, F. Pollmann, G. Salomon, C. Gross, T. A. Hilker, and I. Bloch, Realizing the symmetry-protected Haldane phase in Fermi-Hubbard ladders, Nature (London) **606**, 484 (2022).

[16] F. Anfuso and A. Rosch, String order and adiabatic continuity of Haldane chains and band insulators, Phys. Rev. B **75**, 144420 (2007).

[17] S. Moudgalya and F. Pollmann, Fragility of symmetry-protected topological order on a Hubbard ladder, Phys. Rev. B **91**, 155128 (2015).

[18] S. R. White, Equivalence of the antiferromagnetic Heisenberg ladder to a single $s = 1$ chain, Phys. Rev. B **53**, 52 (1996).

[19] R. Verresen, R. Moessner, and F. Pollmann, One-dimensional symmetry protected topological phases and their transitions, Phys. Rev. B **96**, 165124 (2017).

[20] W. P. Su, J. R. Schrieffer, and A. J. Heeger, Solitons in polyacetylene, Phys. Rev. Lett. **42**, 1698 (1979).

[21] F. D. M. Haldane, Nonlinear field theory of large-spin Heisenberg antiferromagnets: Semiclassically quantized solitons of the one-dimensional easy-axis Néel state, Phys. Rev. Lett. **50**, 1153 (1983).

[22] H. Nonne, E. Boulat, S. Capponi, and P. Lecheminant, Competing orders in the generalized Hund chain model at half filling, Phys. Rev. B **82**, 155134 (2010).

[23] V. Bois, S. Capponi, P. Lecheminant, M. Moliner, and K. Totsuka, Phase diagrams of one-dimensional half-filled two-orbital $SU(N)$ cold fermion systems, Phys. Rev. B **91**, 075121 (2015).

[24] S. Mishra, G. Catarina, F. Wu, R. Ortiz, D. Jacob, K. Eimre, J. Ma, C. A. Pignedoli, X. Feng, P. Ruffieux, J. Fernández-Rossier, and R. Fasel, Observation of fractional edge excitations in nanographene spin chains, Nature (London) **598**, 287 (2021).

[25] J. E. Bunder and H.-H. Lin, Phase diagrams of the metallic zigzag carbon nanotube, Phys. Rev. B **78**, 035401 (2008).

[26] D. Varsano, S. Sorella, D. Sangalli, M. Barborini, S. Corni, E. Molinari, and M. Rontani, Carbon nanotubes as excitonic insulators, Nat. Commun. **8**, 1461 (2017).

[27] C. P. Moca, W. Izumida, B. Dóra, Ö Legeza, J. K. Asbóth, and G. Zaránd, Topologically protected correlated end spin formation in carbon nanotubes, Phys. Rev. Lett. **125**, 056401 (2020).

[28] J. Okamoto, L. Mathey, and W.-M. Huang, Influence of electron-phonon coupling on the low-temperature phases of metallic single-wall carbon nanotubes, Phys. Rev. B **98**, 205122 (2018).

[29] P. W. Anderson, The resonating valence bond state in La_2CuO_4 and superconductivity, Science **235**, 1196 (1987).

[30] P. M. Chaikin and T. C. Lubensky, *Principles of Condensed Matter Physics* (Cambridge University Press, Cambridge, England, 1995).

[31] A. Masayuki and Y. Koichi, Chiral restoration at finite density and temperature, Nucl. Phys. **A504**, 668 (1989).

[32] L. Xu, P. Kumar, S. V. Buldyrev, S.-H. Chen, P. H. Poole, F. Sciortino, and H. E. Stanley, Relation between the widom line and the dynamic crossover in systems with a liquid–liquid phase transition, Proc. Natl. Acad. Sci. U.S.A. **102**, 16558 (2005).

[33] P. Limelette, A. Georges, D. Jérome, P. Wzietek, P. Metcalf, and J. M. Honig, Universality and critical behavior at the Mott transition, Science **302**, 89 (2003).

[34] M. Schüler, E. van Loon, M. Katsnelson, and T. Wehling, Thermodynamics of the metal-insulator transition in the extended Hubbard model, SciPost Phys. **6**, 067 (2019).

[35] J. L. Jiménez, S. P. G. Crone, E. Fogh, M. E. Zayed, R. Lortz, E. Pomjakushina, K. Conder, A. M. Läuchli, L. Weber, S. Wessel, A. Honecker, B. Normand, C. Rüegg, P. Corboz, H. M. Rønnow, and F. Mila, A quantum magnetic analogue to the critical point of water, Nature (London) **592**, 370 (2021).

[36] A. Sushchyev and S. Wessel, Thermodynamics of the metal-insulator transition in the extended Hubbard model from determinantal quantum Monte Carlo, Phys. Rev. B **106**, 155121 (2022).

[37] Y. He, K. Yang, M. O. Goerbig, and R. S. K. Mong, Charge density waves and their transitions in anisotropic quantum Hall systems, Commun. Phys. **4**, 116 (2021).

[38] Y. Zhong, Y. Liu, and H.-G. Luo, Simulating heavy fermion physics in optical lattice: Periodic anderson model with harmonic trapping potential, Front. Phys. **12**, 127502 (2017).

[39] Y. Omori, M. Tsuchiizu, and Y. Suzumura, Mean-field theory of intra-molecular charge ordering in (TTM–TTP)I3, J. Phys. Soc. Jpn. **80**, 024707 (2011).

[40] M. Tsuchiizu, Y. Omori, Y. Suzumura, M.-L. Bonnet, and V. Robert, *Ab initio* derivation of multi-orbital extended Hubbard model for molecular crystals, J. Chem. Phys. **136**, 044519 (2012).

[41] C. P. Landee, M. M. Turnbull, C. Galeriu, J. Giantsidis, and F. M. Woodward, Magnetic properties of a molecular-based spin-ladder system: $(5IAP)_2CuBr_4 \cdot 2H_2O$, Phys. Rev. B **63**, 100402(R) (2001).

[42] V. Bisogni, K. Wohlfeld, S. Nishimoto, C. Monney, J. Trinckauf, K. Zhou, R. Kraus, K. Koepernik, C. Sekar, V. Strocov, B. Büchner, T. Schmitt, J. van den Brink, and J. Geck, Orbital control of effective dimensionality: From spin-orbital fractionalization to confinement in the anisotropic ladder system $CaCu_2O_3$, Phys. Rev. Lett. **114**, 096402 (2015).

[43] Y. Fuseya, M. Tsuchiizu, Y. Suzumura, and C. Bourbonnais, Role of interchain hopping in the magnetic susceptibility of quasi-one-dimensional electron systems, J. Phys. Soc. Jpn. **76**, 014709 (2007).

[44] J.-P. Pouget, Spin-peierls, spin-ladder and kondo coupling in weakly localized quasi-1D molecular systems: An overview, Magnetochemistry **9**, 57 (2023).

[45] S. Hosoi, T. Aoyama, K. Ishida, Y. Mizukami, K. Hashizume, S. Imaizumi, Y. Imai, K. Ohgushi, Y. Nambu, M. Kimata, S. Kimura, and T. Shibauchi, Dichotomy between orbital and magnetic nematic instabilities in $BaFe_2S_3$, Phys. Rev. Res. **2**, 043293 (2020).

[46] S. R. White, Density matrix formulation for quantum renormalization groups, Phys. Rev. Lett. **69**, 2863 (1992).

[47] I. P. McCulloch, Infinite size density matrix renormalization group, revisited, arXiv:0804.2509.

[48] H. N. Phien, G. Vidal, and I. P. McCulloch, Infinite boundary conditions for matrix product state calculations, Phys. Rev. B **86**, 245107 (2012).

[49] J. Haegeman, C. Lubich, I. Oseledets, B. Vandereycken, and F. Verstraete, Unifying time evolution and optimization with matrix product states, Phys. Rev. B **94**, 165116 (2016).

[50] V. Zauner-Stauber, L. Vanderstraeten, M. T. Fishman, F. Verstraete, and J. Haegeman, Variational optimization algorithms for uniform matrix product states, Phys. Rev. B **97**, 045145 (2018).

[51] I. P. McCulloch, From density-matrix renormalization group to matrix product states, J. Stat. Mech. (2007) P10014.

[52] U. Schollwöck, The density-matrix renormalization group in the age of matrix product states, Ann. Phys. (N.Y.) **326**, 96 (2011), January 2011 Special Issue.

[53] G. Karakonstantakis, E. Berg, S. R. White, and S. A. Kivelson, Enhanced pairing in the checkerboard Hubbard ladder, Phys. Rev. B **83**, 054508 (2011).

[54] M. Dolfi, B. Bauer, S. Keller, and M. Troyer, Pair correlations in doped Hubbard ladders, Phys. Rev. B **92**, 195139 (2015).

[55] Y. Shen, G.-M. Zhang, and M. Qin, Reexamining doped two-legged Hubbard ladders, Phys. Rev. B **108**, 165113 (2023).

[56] Z. Zhou, W. Ye, H.-G. Luo, J. Zhao, and J. Chang, Robust superconducting correlation against intersite interactions in the extended two-leg Hubbard ladder, Phys. Rev. B **108**, 195136 (2023).

[57] Z. Weihong, J. Oitmaa, C. J. Hamer, and R. J. Bursill, Numerical studies of the two-leg Hubbard ladder, J. Phys. Condens. Matter **13**, 433 (2001).

[58] C. Yang and A. E. Feiguin, Spectral function of Mott-insulating Hubbard ladders: From fractionalized excitations to coherent quasiparticles, Phys. Rev. B **99**, 235117 (2019).

[59] M. Vojta, R. E. Hetzel, and R. M. Noack, Charge-order transition in the extended Hubbard model on a two-leg ladder, Phys. Rev. B **60**, R8417 (1999).

[60] N. J. Robinson, F. H. L. Essler, E. Jeckelmann, and A. M. Tsvelik, Finite wave vector pairing in doped two-leg ladders, Phys. Rev. B **85**, 195103 (2012).

[61] E. Orignac and R. Citro, Charge density waves and bond orderwaves in a quarter filled extended Hubbard ladder, Eur. Phys. J. B **33**, 419 (2003).

[62] M. Tsuchiizu and Y. Suzumura, Charge-density-wave formation in the doped two-leg extended Hubbard ladder, J. Phys. Soc. Jpn. **73**, 804 (2004).

[63] M. M. Rams, P. Czarnik, and L. Cincio, Precise extrapolation of the correlation function asymptotics in uniform tensor network states with application to the Bose-Hubbard and XXZ models, Phys. Rev. X **8**, 041033 (2018).

[64] See Supplemental Material at http://link.aps.org/supplemental/10.1103/PhysRevLett.132.136501 for data extrapolation for correlation lengths shown in the main text and the mentioned exponents of singlet density difference correlation functions. Additional data is provided for excitations gaps and spectral functions. Detailed theoretical analysis of the microscopic model and the effective theory is provided.

[65] E. Lieb, T. Schultz, and D. Mattis, Two soluble models of an antiferromagnetic chain, Ann. Phys. (N.Y.) **16**, 407 (1961).

[66] H. Tasaki, Lieb-Schultz-Mattis theorem with a local twist for general one-dimensional quantum systems, J. Stat. Phys. **170**, 653 (2018).

[67] I. Affleck, T. Kennedy, E. H. Lieb, and H. Tasaki, Rigorous results on valence-bond ground states in antiferromagnets, Phys. Rev. Lett. **59**, 799 (1987).

[68] A. Prakash, M. Fava, and S. A. Parameswaran, Multiversality and unnecessary criticality in one dimension, Phys. Rev. Lett. **130**, 256401 (2023).

[69] H. Yao and S. A. Kivelson, Fragile Mott insulators, Phys. Rev. Lett. **105**, 166402 (2010).